

MIT Open Access Articles

Fluorescence-Based Nitric Oxide Sensing by Cu(II) Complexes That Can Be Trapped in Living Cells

The MIT Faculty has made this article openly available. **Please share** how this access benefits you. Your story matters.

Citation: McQuade, Lindsey E., and Stephen J. Lippard. "Fluorescence-Based Nitric Oxide Sensing by Cu(II) Complexes That Can Be Trapped in Living Cells." *Inorganic Chemistry* 49.16 (2010): 7464-7471.

As Published: <http://dx.doi.org/10.1021/ic100802q>

Publisher: American Chemical Society

Persistent URL: <http://hdl.handle.net/1721.1/67684>

Version: Author's final manuscript: final author's manuscript post peer review, without publisher's formatting or copy editing

Terms of Use: Article is made available in accordance with the publisher's policy and may be subject to US copyright law. Please refer to the publisher's site for terms of use.



Fluorescence-Based Nitric Oxide Sensing by Cu(II) Complexes that Can Be Trapped in Living Cells

*Lindsey E. McQuade and Stephen J. Lippard**

Contribution from the Department of Chemistry, Massachusetts Institute of Technology, Cambridge,
Massachusetts 02139

Email: lippard@mit.edu

RECEIVED DATE

TITLE RUNNING HEAD: Nitric Oxide Sensing by Cu(II) Complexes

ABSTRACT: A series of symmetrical, fluorescein-derived ligands appended with two derivatized 2-methyl-8-aminoquinolines were prepared and spectroscopically characterized. The ligands FL2, FL2E, and FL2A were designed to improve the dynamic range of previously described asymmetric systems, and the copper complex Cu₂(FL2E) was constructed as a trappable NO probe that is hydrolyzed intracellularly to form Cu₂(FL2A). The ligands themselves are only weakly emissive, and the completely quenched Cu(II) complexes, generated in situ by combining each ligand with two equivalents of CuCl₂, were investigated as fluorescent probes for nitric oxide. Upon introduction of excess NO under anaerobic conditions to buffered solutions of Cu₂(FL2), Cu₂(FL2E), and Cu₂(FL2A), the fluorescence increased by factors of 23 ± 3 , 17 ± 2 , and 27 ± 3 , respectively. The corresponding rate constants for fluorescence turn-on were determined to be $0.4 \pm 0.2 \text{ min}^{-1}$, $0.35 \pm 0.05 \text{ min}^{-1}$ and $0.6 \pm 0.1 \text{ min}^{-1}$. The

probes are highly specific for NO over other biologically relevant reactive oxygen and nitrogen species, as well as Zn(II), the metal ion for which similar probes were designed to detect.

KEYWORDS: Biological signaling, cell-trappable sensor, fluorescence

Introduction

Since the discovery that nitric oxide (NO) is the endothelium derived relaxation factor (EDRF) responsible for vascular smooth muscle dilation,¹⁻³ NO has been implicated as a biological signaling agent in a wide variety of physiological processes, ranging from roles in the immune system⁴ to neurotransmission⁵ to cardiovascular function.⁶ Like any secondary messenger, regulation is key to maintaining homeostasis, and failure to regulate NO production is associated with pathologies including cancer, neurodegeneration, sepsis, and stroke.⁶

In order to elucidate the exact function of nitric oxide in vivo, it is valuable to have sensitive, selective tools for its detection. There are many techniques available for NO sensing, such as colorimetry, chemiluminescence, electron paramagnetic resonance (EPR), and electrochemistry,⁷ but the many advantages of fluorescence microscopy render it among the most valuable options to date. Fluorescent probes can be made to detect analytes of interest rapidly, directly, and selectively. When they are synthesized to be water soluble, non-toxic, and membrane permeable, they can enter living cells and report on the generation and translocation of the analyte. When chemistry occurs to turn them on or off, striking luminescent changes can ensue. The ability to track NO by fluorescence inside cells has the potential to revolutionize our understanding of its biology by supplying researchers with important information about the subcellular processes it affects. Toward this end, NO probes have been constructed out of small molecules, polymers,⁸⁻¹¹ nanotubes,¹² proteins,¹³ and even whole cells.^{14,15}

Transition metal complexes have also been investigated as platforms for NO detection,¹⁶ because NO can react directly and potentially reversibly with metal centers.¹⁷ When designing metal-based turn-on

fluorescent probes, either the paramagnetism of the metal or the heavy atom effect will serve to quench the fluorescence of an appended fluorophore. This task can be accomplished by incorporation of the fluorophore into the ligand such that it is in close proximity to the metal center. Restoration of fluorescence is accomplished either by removing the fluorophore from the metal, typically by metal-nitrosyl formation to displace the ligand, by reduction of a paramagnetic metal to a diamagnetic redox state, or both. Metal-based probes have been designed using a variety of ligand scaffolds, and a spectrum of metals that include Fe(II),^{18,19} Co(II),^{18,20-22} Cu(II),²³⁻²⁹ Ru(II),^{30,31} and Rh(II).^{32,33}

Previously, we described the synthesis and application of a derivatized fluorescein, FL1 (Figure 1a), which forms a 1:1 complex with Cu(II). This complex reacts with nitric oxide to evolve chemistry leading to fluorescence enhancement through nitrosation of the secondary amine on the ligand.²³ CuFL1 responds directly and selectively to NO, exhibiting a dramatic fluorescence enhancement. Although details of the intimate mechanism are still under investigation, the overall product of the reaction of CuFL1 with NO is the *N*-nitrosated ligand, FL1-NO, the species responsible for fluorescence turn-on (Figure 1b). In addition to being an excellent NO sensor *in vitro*, CuFL1 can detect endogenously produced NO in cell culture.^{24,34-39} The probe has excellent biocompatibility, being water soluble, non-toxic, and cell membrane permeable. Because fluorescein is the emitter, CuFL1 is excited by relatively low energy light, and the emissive final product after reaction with NO is green. For CuFL1 to be useful for experiments in biological tissues and animals, for which continual fluid perfusion is required, it must be retained within cells. Unfortunately, under perfusion conditions CuFL1 diffuses out of cells. The inability to retain the probe within cells under such conditions inspired the present work to create a trappable version. Several synthetic strategies were explored, and the most successful derivative was that in which two Cu(II) binding units, incorporating esters as the trappable moieties, were installed onto a xanthone ring. The esters maintain the cell membrane permeability of the probes until inside the cell, at which point intracellular esterases hydrolyze the esters to produce negatively charged carboxylate func-

tionalities.⁴⁰ The negative charge prevents the probe from re-crossing cell membranes, rendering it trapped within the cell.

Herein we report the synthesis and photophysical characterization of three new ligands, FL2, FL2E, and FL2A. These symmetrical, second-generation ligands are based on FL1, and FL2E employs the ester/acid strategy for cell-trappability. Their copper(II) complexes, generated in situ, respond quickly and selectively to nitric oxide over other biologically relevant reactive oxygen and nitrogen species (RONS). As described elsewhere, the probes have detected NO production in stimulated mouse brain olfactory bulb tissue slices.⁴¹

Experimental Section

Synthetic Materials and Methods. Anhydrous methanol (Aldrich) was used as received. 8-Aminoquinoline,⁴² 4',5'-fluoresceindicarboxaldehyde,⁴³ 2-{4,5-bis[(6-(2-ethoxy-2-oxoethoxy)-2-methylquinolin-8-ylamino)-methyl]-6-hydroxy-3-oxo-3*H*-xanthen-9-yl}benzoic acid (FL2E),⁴¹ and 2,2'-{8,8'-[9-(2-carboxyphenyl)-6-hydroxy-3-oxo-3*H*-xanthene-4,5-diyl]bis(methylene)bis(azanediyl)-bis(2-methylquinolin-8,6-diyl)}-bis(oxy)diacetic acid (FL2A)⁴¹ were prepared by previously reported procedures. Sodium borohydride (Sigma), sodium hydroxide (Mallinckrodt Chemicals), and all deuterated solvents (Cambridge Isotope Laboratories) were used as received. Silica gel (SiliaFlash F60, Silicycle, 230-400 mesh) was used for column chromatography. Thin-layer chromatography (TLC) was performed on EMD Chemicals F254 silica gel-60 plates (1 mm thickness) and viewed by either UV light or ninhydrin staining. ¹H and ¹³C{¹H} NMR spectra were obtained on either a Varian 300 MHz or 500 MHz spectrometer and referenced to the residual proton or carbon resonance of the deuterated solvent. High-resolution mass spectra were measured by staff at the MIT Department of Chemistry Instrumentation Facility (DCIF).

2-{6-Hydroxy-4,5-bis[(2-methylquinolin-8-ylamino)methyl]-3-oxo-3*H*-xanthen-9-yl}benzoic acid (1, FL2). 4',5'-Fluoresceindicarboxaldehyde (115 mg, 296 μmol) and 8-aminoquinoline (107 mg, 676

μmol) were suspended in methanol (12 mL) and stirred at room temperature for 1 h. The dark red-purple suspension was cooled to 0 °C and sodium borohydride (86.3 mg, 2.28 mmol) was added. The reaction clarified to a dark red solution and was stirred for 1 h as it warmed to room temperature. The solvent was removed and the resulting residue was purified by column chromatography on silica (gradient from 100% CH_2Cl_2 to 19:1 CH_2Cl_2 : CH_3OH) to afford a dark red solid (100 mg, 50%). TLC R_f = 0.71 (silica, 9:1 CH_2Cl_2 : CH_3OH); mp: 164-165 °C (dec); ^1H NMR (CD_3OD + drops of CD_2Cl_2 , 300 MHz): δ 2.56 (6H, s), 4.78 (4H, s), 6.56 (2H, d, J = 8.7 Hz), 6.63 (2H, d, J = 8.7 Hz), 6.82 (2H, dd, J = 7.7 Hz, 1.1 Hz), 6.93 (2H, dd, J = 8.3, 1.1 Hz), 7.09 – 7.18 (5H, m), 7.61 – 7.71 (2H, m), 7.88 (2H, d, J = 8.4 Hz), 7.98 (1H, dd, J = 6.3, 1.3 Hz); $^{13}\text{C}\{^1\text{H}\}$ NMR ($\text{DMSO}-d_6$, 125 MHz): δ 25.90, 37.20, 106.04, 111.05, 113.43, 114.79, 123.21, 123.46, 125.34, 125.86, 127.43, 127.52, 127.67, 127.85, 128.81, 131.32, 136.71, 137.39, 138.09, 144.83, 151.62, 153.15, 156.50, 158.88, 169.70; HRMS (m/z): $[\text{M} - \text{H}]^-$ calcd 671.2300, found 671.2283; Anal. Calcd for $\text{C}_{42}\text{H}_{32}\text{N}_4\text{O}_5 \cdot \text{H}_2\text{O}$: C, 73.03; H, 4.96; N, 8.11; Found: C, 72.91; H, 5.17; N, 8.09.

Spectroscopic Materials and Methods. Piperazine- N,N' -bis(2-ethanesulfonic acid) (PIPES) was purchased from Calbiochem. Potassium chloride (99.999%) was purchased from Aldrich. Buffer solutions (50 mM PIPES, 100 mM KCl, pH 7) were prepared in Millipore water and used for all spectroscopic measurements except for pK_a titrations, which were performed in a solution of 10 mM KOH, 100 mM KCl, pH 12 in Millipore water. The pH of the solutions was adjusted to the desired values using 6, 1, or 0.1 N HCl and 0.1 N KOH. Quantum yields were measured using fluorescein in 0.1 N NaOH (ϕ = 0.95) as the standard.⁴⁴ Nitric oxide was purchased from Airgas and purified as previously described.⁴⁵ *S*-Nitroso-*N*-acetyl-DL-penicillamine (SNAP, Cayman Chemical), potassium nitrate (Aldrich), sodium nitrite (Aldrich), sodium peroxyxynitrite (Cayman Chemical), Angeli's salt ($\text{Na}_2\text{N}_2\text{O}_3$, Cayman Chemical), hydrogen peroxide (Mallinckrodt Chemicals), and sodium hypochlorite (J. T. Baker) were prepared as 50 mM stock solutions in Millipore water. Nitric oxide and other reactive oxygen and nitrogen species (RONS) were introduced into buffered solutions via gas tight syringes. Copper chloride dihydrate

(99+%) was purchased from Alfa Aesar and stock solutions of 10 mM and 1 mM were prepared in Millipore water. Zinc chloride (Aldrich, 99.999%) stock solutions of 100 mM and 1 mM were prepared in Millipore water. Stock solutions of 1 mM ligands were prepared in DMSO and stored in aliquots at -80 °C. UV-visible spectra were acquired on a Cary 50-Bio spectrometer using PMMA cuvettes from Perfeq Science (3.5 mL volume, 1 cm path length). Acquisitions were made at 25.00 ± 0.05 °C. Fluorescence spectra were obtained on a Quanta Master 4 L-format scanning spectrofluorimeter (Photon Technology International) at 37.0 ± 0.1 °C using $1 \mu\text{M}$ $\text{Cu}_2(\text{L})$ (L = FL2, FL2E or FL2A) generated in situ by combining stock solutions of CuCl_2 and L in a 2:1 ratio, and then introducing either 1.3 mM NO or 167 μM RONS. Fluorescence measurements were made under anaerobic conditions, with cuvette solutions prepared in an inert atmosphere glove box. Replicate fluorescence measurements were taken at time points between 40 s and 60 min.

Results and Discussion

Design Considerations. The reported probes are based on the CuFL1 scaffold, a first-generation sensor with many beneficial features. Fluoresceins are bright, with fluorescence quantum yields approaching unity,⁴⁴ but the aminoquinoline unit of FL1 quenches emission by photoinduced electron transfer (PeT) in the excited state.²³ CuFL1 is also quenched owing to its paramagnetic Cu(II) center, and emission is restored upon reduction of Cu(II) to Cu(I) with concomitant formation of FL1-NO (Fig. 1). The

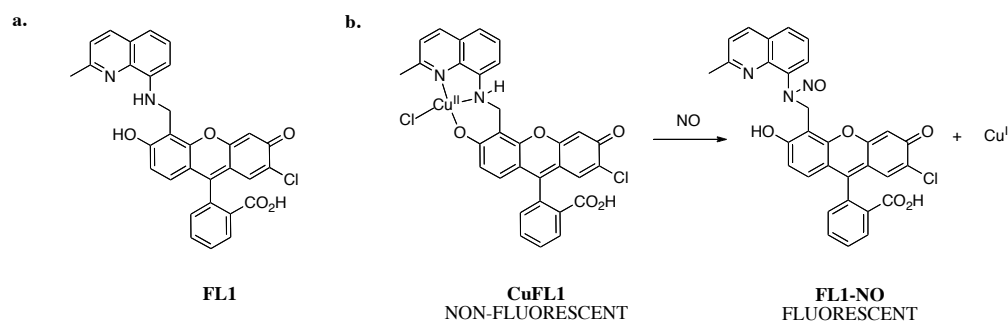
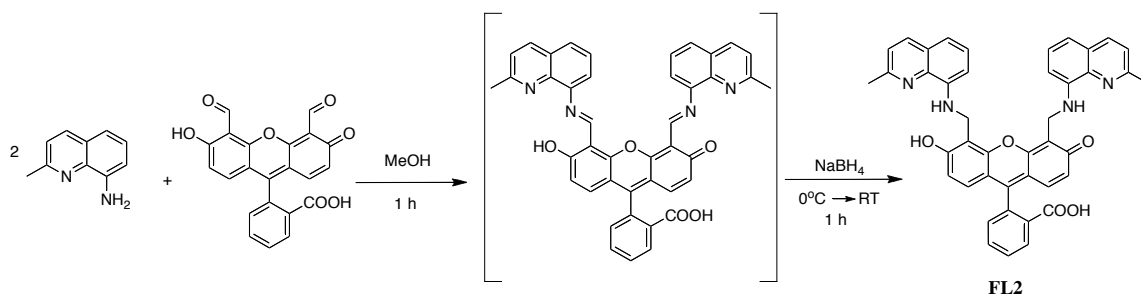


Figure 1. a) Structure of FL1 and b) NO CuFL1 and its NO detection scheme.

tridentate N_2O donor set of the ligand coordinates Cu(II) with moderate affinity ($K_d = 1.5 \mu\text{M}$) but cannot retain Cu(I), possibly due to its inability to

support a tetrahedral geometry, its hard donor atoms, and the reduced affinity of the nitrosated amine for copper.^{23,24} Moving from FL1 to a symmetric scaffold offers two main advantages. Firstly, it avoids the more laborious synthesis of 7'-chloro-4'-fluorescein carboxaldehyde in favor of the simpler symmetric variant.^{46,47} Secondly, symmetric ligands tend to have lower fluorescence quantum yields than their asymmetric derivatives, probably because of the extra lone pair(s) of electrons, one of which is delocalized over the aminoquinoline unit, available for PeT quenching of the excited fluorophore.⁴⁸ Moreover, Cu(II) chelation on both ligand arms should force lactonization of the bottom ring benzoic acid to produce two phenolic oxygen atoms for superior metal binding, decreasing emission by disrupting conjugation of the fluorophore. These features will produce a more quenched ligand, increasing the dynamic range of emission upon exposure to NO. An acetoxyethyl ester was employed because the negatively charged carboxylic acid product of its hydrolysis is not rapidly effluxed by the cell unlike the commonly used fluorescein acetate esters, which yield the basic fluorescein scaffold upon hydrolysis and are subsequently removed from the intracellular environment more rapidly.⁴⁹

Synthesis. The synthesis of FL2 is depicted in Scheme 1. Condensation of 8-aminoquinoline with 4',5'-fluorescein dialdehyde in a 2:1 ratio in methanol followed by reduction using sodium borohydride afforded FL2 in good yield. The ligand was purified by column chromatography on silica, a major improvement over the purification of asymmetric FL1,²³ which required preparative TLC. The syntheses of FL2E and FL2 are reported elsewhere.⁴¹ FL2E was obtained in moderate yield in a manner analogous to



Scheme 1. Synthesis of FL2.

that used for FL2, employing ethyl[(8-amino-2-methylquinolin-6-yloxy)acetate] as the quinoline. Hydrolysis of FL2E gives FL2 in excellent yield, without the need for additional purification steps.

Spectroscopic Properties of FL2, FL2E and FL2A. Table 1 summarizes the spectroscopic properties of the FL2, FL2E, FL2A, and their corresponding dicopper derivatives. Previously reported spectroscopic properties of the first generation ligands and sensors are included for comparison.^{23,24} The absorption spectra of the ligands are typical of those in fluorescein-derived species, exhibiting maxima at 498 nm ($\epsilon = 2.91 \pm 0.07 \times 10^4 \text{ M}^{-1}\text{cm}^{-1}$), 500 nm ($\epsilon = 1.79 \pm 0.07 \times 10^4 \text{ M}^{-1}\text{cm}^{-1}$), and 499 nm ($\epsilon = 4.60 \pm 0.06 \times 10^4 \text{ M}^{-1}\text{cm}^{-1}$) for FL2, FL2E and FL2A, respectively. Titrations of buffered solutions of the ligands with CuCl_2 revealed the binding stoichiometries of each probe (Figure S1). When one and two equivalents of Cu(II) are added to buffered solutions of FL2 and FL2E, the absorbance at λ_{max} decreases. Upon addition of further equivalents of Cu(II) the absorbance at λ_{max} remains constant. This result is expected for the binding of two copper atoms by the two N_2O donor sets. When the same experiment is performed using FL2A, there is a decrease in absorbance at λ_{max} upon addition of one, two, and three equivalents of Cu(II), with no further changes upon titrating additional equivalents of Cu(II). The three events probably correspond to two copper binding steps at the two N_2O donor sites and a third binding at the upper-ring acids. Upon addition of two equivalents of CuCl_2 , the absorbance maxima blue shift to 494 nm ($\epsilon = 1.14 \pm 0.07 \times 10^4 \text{ M}^{-1}\text{cm}^{-1}$), 496 nm ($\epsilon = 1.12 \pm 0.06 \times 10^4 \text{ M}^{-1}\text{cm}^{-1}$) and 495 nm ($\epsilon = 1.56 \pm 0.02 \times 10^4 \text{ M}^{-1}\text{cm}^{-1}$), for FL2, FL2E and FL2A, respectively. These blue shifts are presumably due to

Table 1. Photophysical properties of FL2, FL2E, and FL2A.

	Absorbance λ (nm), $\epsilon \times 10^4$ ($\text{M}^{-1}\text{cm}^{-1}$)		Emission λ (nm), ϕ (%) ^b				ref
	unbound	Cu(II)	unbound	Cu(II)	+ NO	DR ^c	
FL ₁ ^a	504, 4.3(1)	499, 4.0(1)	520, 8.3(4)	520, nr ^d	nr, nr	2.5(1)	7
FL ₂	503, 3.8(5)	496, 3.8(3)	520, 8.4(2)	520, nr	nr, nr	8.3(9)	7
FL ₃	503, 3.9(1)	497, 3.9(5)	520, 31(1)	520, nr	nr, nr	3.4(1)	7
FL ₄	505, 6.9(1)	496, 5.7(1)	520, 2.4(2)	520, nr	nr, nr	31(1)	7
FL1	504, 4.2(1)	499, 4.0(1)	520, 7.7(2)	520, nr	526, 58(2)	16(1)	7, 10
FL2	498, 2.91(7)	494, 1.14(7)	515, 0.74(5)	512, 0.76(4)	526, 51(7)	23(3)	this work
FL2E	500, 1.79(7)	496, 1.06(6)	522, 0.37(5)	522, 0.72(4)	526, 40(8)	17(2)	this work, 16
FL2A	499, 4.6(6)	495, 1.56(2)	516, 1.8(2)	516, 1.9(2)	526, 36(5)	27(3)	this work, 16

^a Measurements were performed in 50 mM PIPES, 100 mM KCl, pH 7.0, T = 25 °C. ^b Referenced to fluorescein ($\phi = 0.95$ in 0.1 N NaOH). ^c DR is the dynamic range, I_{NO}/I_0 . ^d nr is not reported.

perturbation of the xanthenone ring π -system, which occurs when Cu(II) binds to the phenolic oxygen atoms of fluorescein.

NO Reactivity of the Copper-Ligand Complexes. The free ligands, FL2, FL2E, and FL2A emit with maxima at 515, 522, and 516 nm, respectively, and undergo minimal changes upon binding Cu(II). The quantum yields of the ligands are $0.74 \pm 0.05\%$, $0.37 \pm 0.05\%$ and $1.8 \pm 0.2\%$ for FL2, FL2E, and FL2A, respectively. By comparison, the quantum yield for FL1 is $7.7 \pm 0.2\%$. Because the extinction

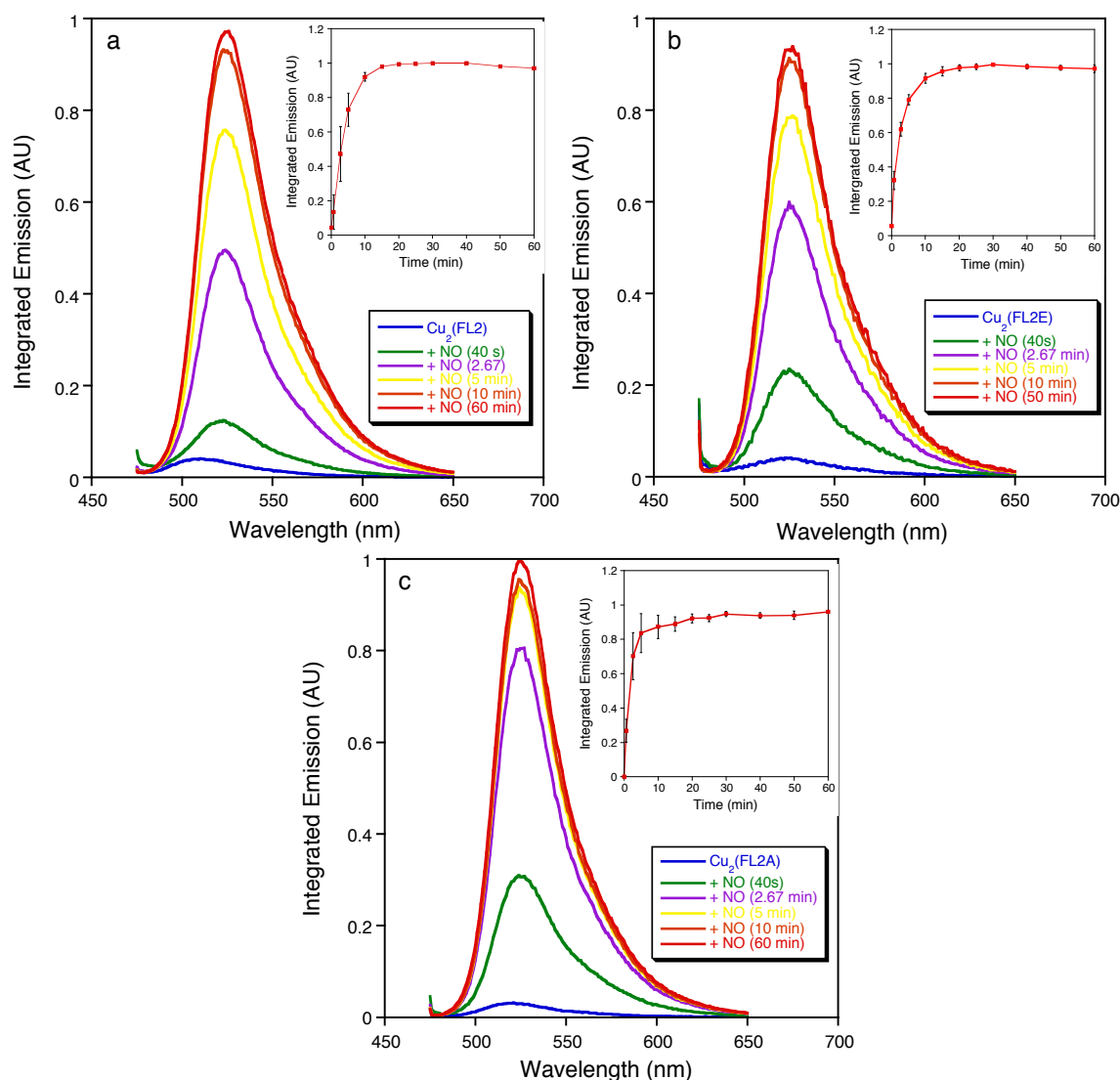
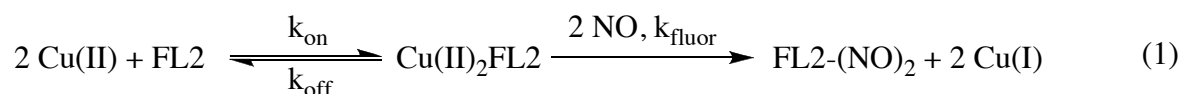


Figure 2. Normalized fluorescence response of a) Cu₂(FL2), b) Cu₂(FL2E), and c) Cu₂(FL2A) in the presence of excess NO over 1 h in 50 mM PIPES, 100 mM KCl, pH 7.0, T = 37 °C. Insets: Plots of integrated fluorescence vs. time, normalized and adjusted for the basal fluorescence of the sensor in the absence of NO.

coefficients of the symmetric ligands are also lower than that of FL1, incorporation of a second quench-

ing unit brings about a striking decrease in brightness for the free ligand, where brightness is $\epsilon \times \Phi$. Coordination to Cu(II) does not appreciably alter the quantum yields of the ligands (Table 1), whereas significant ($18 \pm 3\%$) quenching occurs when FL1 binds Cu(II). This result suggests that the additional quenching provided by the second aminoquinoline unit compensates for that provided by coordination to a paramagnetic center. Buffered solutions of probes generated in situ by combining CuCl_2 and ligand in a 2:1 ratio exhibit significant fluorescence enhancements relative to that of the initial copper complexes when exposed to excess NO under anaerobic conditions (Figure 2, Tables 1). In all cases, the fluorescence enhancement matches ($\text{Cu}_2(\text{FL2E})$) or greatly exceeds ($\text{Cu}_2(\text{FL2})$ and $\text{Cu}_2(\text{FL2A})$) that of CuFL1 (Table 1). Accompanying the fluorescence enhancement is a red-shift of the emission maxima to 526 nm for all probes, which is consistent with formation of the free, *N*-nitrosated derivatives of the ligands.^{23,24} Also consistent with *N*-nitrosation are the increased quantum yields of the final solutions after complete reaction with NO (Table 1). The reaction of the probes with NO can also be monitored by the change in absorption over time. Probe solutions exposed to NO under anaerobic conditions were monitored over the course of an hour, during which time the λ_{max} value red-shifted to 504 nm for all probes (Figure S2).

Kinetics of NO reactivity. The approximate rate of fluorescence enhancement upon reaction of the probes with NO was determined using the fluorescence data from the previous section. The reaction occurs in two kinetic phases, characterized by a pre-equilibrium of Cu(II) binding and then an irreversible



reaction of the Cu(II) complex with NO (eq. 1). The reaction for each probe with NO was monitored multiple times by fluorescence, and the plots of the fluorescence enhancement over time were fit to the expression $y = Ae^{(-x/t)} + y_0$ to obtain k_{fluor} (Figure 3). This analysis gave estimates for the rate constants of NO reactivity of $0.4 \pm 0.2 \text{ min}^{-1}$, $0.35 \pm 0.05 \text{ min}^{-1}$ and $0.6 \pm 0.1 \text{ min}^{-1}$ for $\text{Cu}_2(\text{FL2})$, $\text{Cu}_2(\text{FL2E})$ and

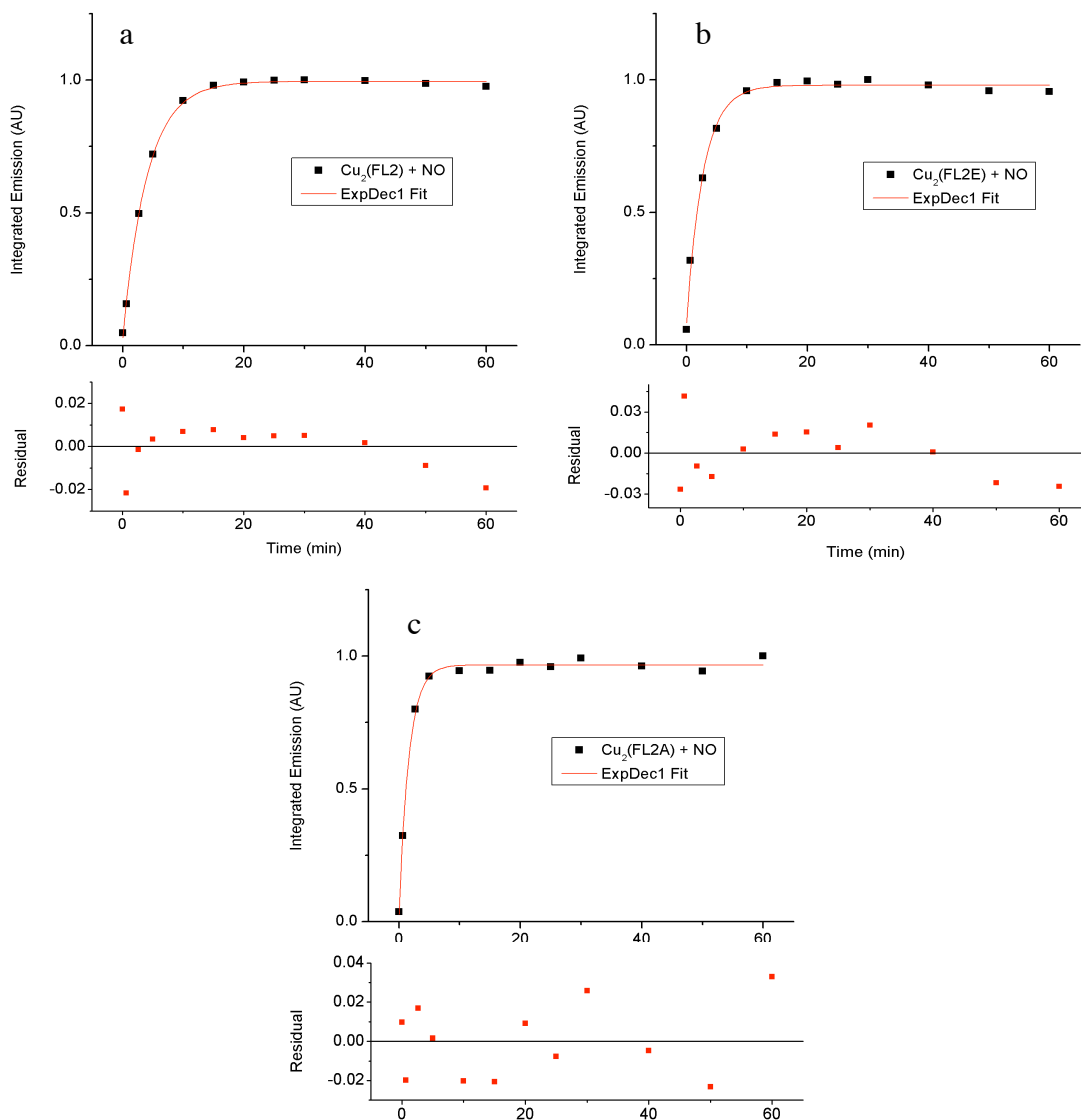


Figure 3. Plots of integrated fluorescence vs. time and residual plots of the exponential fits applied to the fluorescence vs. time graphs for the reaction of a) 1 μM $\text{Cu}_2(\text{FL2})$, b) 1 μM $\text{Cu}_2(\text{FL2E})$, and c) 1 μM $\text{Cu}_2(\text{FL2A})$ with 1.3 mM NO in 50 mM PIPES, 100 mM KCl, pH 7.0, $T = 37^\circ\text{C}$, normalized and adjusted for the basal fluorescence of the sensor in the absence of NO.

$\text{Cu}_2(\text{FL2A})$, respectively. A more detailed kinetic and mechanistic analysis is in progress and will be reported elsewhere.

Probe selectivity. The reaction of the probes with NO is not limited to the gaseous form of the molecule. A fluorescence response is also observed when the probes are exposed to *S*-nitrosothiols such as *S*-nitroso-*N*-acetyl-DL-penicillamine (SNAP, Table 2). Because of the diversity of NO reactions under biological conditions, it is imperative that NO probes are selective for molecule itself and not its oxidation products, including NO_2^- and NO_3^- , products of NO reactions, including ONOO^- and HNO, or other

cellular oxidizing species, such as H_2O_2 or ClO^- . When these biologically relevant reactive oxygen and nitrogen species (RONS) are introduced to buffered probe solutions, the fluorescence enhancement over 1 h is minimal by comparison to that afforded by NO (Figure 4, Table 2). This result is consistent with the chemistry of the first generation probe $\text{CuFL1}^{23,24}$ and indicates that modifications to the quinoline moiety do not interfere with the selectivity of the probes to sense nitric oxide or other NO-transfer agents such as *S*-nitrosothiols.

Table 2. Selectivity of $\text{Cu}_2(\text{FL2})$, $\text{Cu}_2(\text{FL2E})$ and $\text{Cu}_2(\text{FL2A})$ for NO over other RONS after 1 h.

RONS	Fluorescence Enhancement (F/F_0)		
	$\text{Cu}_2(\text{FL2})^a$	$\text{Cu}_2(\text{FL2E})$	$\text{Cu}_2(\text{FL2A})$
NO	23(3)	17(2)	27(3)
SNAP	18(1)	10(1)	15(3)
NO_2^-	0.92(8)	1.17(6)	1.56(4)
NO_3^-	0.84(2)	0.92(1)	1.33(4)
H_2O_2	1.3(1)	1.8(2)	4(1)
ClO^-	1.5(2)	1.26(9)	1.8(2)
ONOO^-	1.40(7)	1.2(2)	4(1)
HNO^b	1.4(1)	1.3(2)	1.3(2)

^a Measurements were performed in 50 mM PIPES, 100 mM KCl at pH 7.0, 37 °C, 1 h, 100 equiv. RONS. ^b HNO is generated from Angeli's salt, $\text{Na}_2\text{N}_2\text{O}_3$.

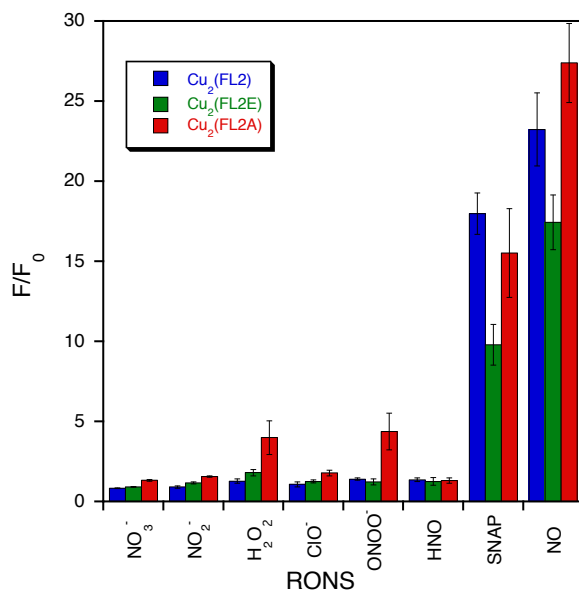


Figure 4. Selectivity of 1 μM $\text{Cu}_2(\text{FL2})$, 1 μM $\text{Cu}_2(\text{FL2E})$, and 1 μM $\text{Cu}_2(\text{FL2A})$ for NO over other RONS (167 μM). Normalized fluorescence response after 1 h relative to the emission of the probe in 50 mM PIPES, 100 mM KCl, pH 7.0, T = 37 °C.

pH Dependence. The emission of the ligands depends on pH, and this dependence was investigated by fluorescence and UV-visible spectroscopy for FL2 and FL2A only, because FL2E hydrolyzes under the experimental conditions. Starting at pH 12, addition of protons to either ligand results in a fluorescence enhancement that is marginal until \sim pH 8 (FL2) or pH 9 (FL2A), but then increases sharply until \sim pH 6 for both (Figure 5). By comparison to the fluorescence enhancement induced by reaction of $\text{Cu}_2(\text{FL2})$ or $\text{Cu}_2(\text{FL2A})$ with NO, protonation of FL2 or FL2A causes only an approximate 2-fold fluorescent enhancement. This result indicates the ligands are fairly insensitive to pH in the biologically relevant range of \sim 6 – 8, especially by comparison to NO-promoted fluorescence. Further lowering of the pH results in a steep decrease in fluorescence for both ligands, probably due to protonation of the fluorescein, which forms non-fluorescent species.⁵⁰ The first set of pK_a values were obtained by fitting the UV-vis data (Figure S3), revealing values of \sim 7.0 and \sim 5.9 for FL2 and FL2A, respectively. Because there are multiple protonation sites on each ligand, but only one pK_a value was obtained from the absorption titration, the numbers represent an average pK_a for each ligand. The second set of pK_a values were returned by fitting the fluorescence data (Figure S4). Three values were obtained for each ligand. The first, \sim 7.3 and \sim 7.9 for FL2 and FL2A, respectively, is attributed to protonation of the secondary amine nitrogen atoms.⁴⁸ Because protonation breaks the symmetry of the ligand, there should be two pK_a

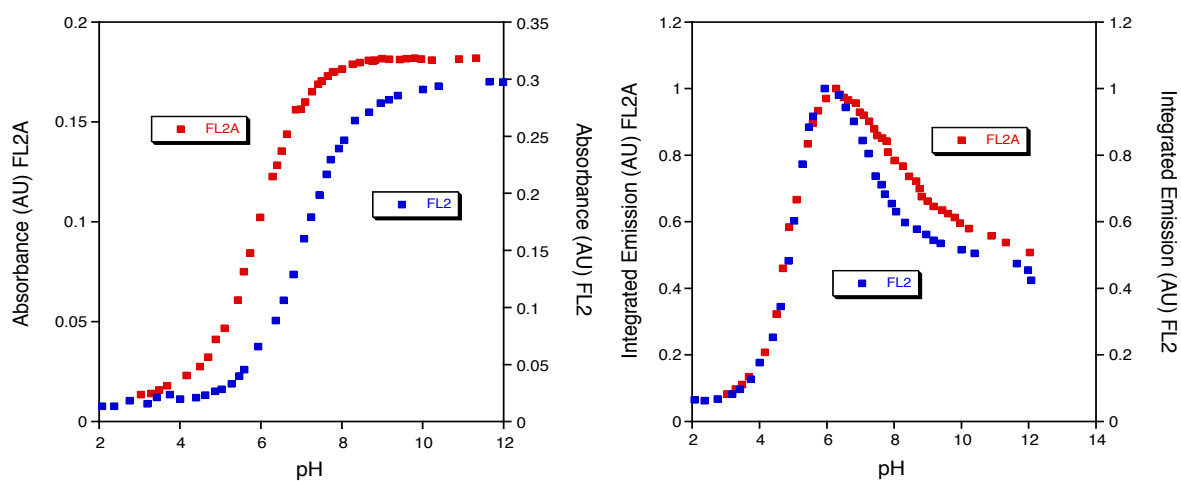


Figure 5. Absorbance (left) and fluorescence emission (right) dependence on pH for 5 μM FL2 and 5 μM FL2A in 10 mM KOH, 100 mM KCl, pH \sim 12, T = 25 $^{\circ}\text{C}$. pH adjusted with 6 N, 1 N and 0.1 N HCl and 0.1 N KOH.

values in these regions. The first fluorescence value should therefore be treated as an apparent pK_a . The second fluorescence pK_a value, ~ 5.9 and ~ 6.2 for FL2 and FL2A, respectively, corresponds to the maximum of the titration curves and can be attributed to protonation of the quinoline ring. The third fluorescence pK_a value, which is most likely a combination of fluorescein carboxylic acid protonation and lactonization events, is 5.0 and 4.9, for FL2 and FL2A, respectively. It was determined by fitting the fluorescence plots from \sim pH 6 (the maxima) to the lowest pH values.

Excess Zn(II) Does Not Turn on the Cu(II)-Ligand Complexes. Zinc ions are ubiquitous in biology, providing structural support and performing catalytic roles in a variety of proteins.⁵¹ In such proteins, Zn(II) is tightly bound and, in general, intracellular zinc concentrations are closely regulated by Zn(II)-specific transporters, such as ZnT-3, and Zn(II)-binding proteins, such as metallothionein (MT).⁵² Through NO reactivity it is possible for Zn(II) to be released from proteins. For example, NO nitrosates the Zn(II)-binding cysteines in MT, which results in loss of Zn(II) from the protein and an increase in local Zn(II) concentration.⁵³

The design of CuFL1 probe is similar to that of the Zn(II) probe QZ1, which contains a similar N_2O metal-binding pocket.⁴⁸ QZ1 binds Zn(II) selectively over Na(I), Ca(II), Mg(II), Mn(II), Fe(II), Co(II), Cd(II) and Hg(II); however, Ni(II) and Cu(II) compete, a result obtained from an experiment using a 50:1 M(II):QZ1 ratio. We therefore considered, in the present context, whether excess Zn(II) might displace Cu(II) from the probes, thereby causing fluorescence enhancement. To investigate this possibility, the fluorescence of the probes was monitored before and after the addition of $ZnCl_2$ (Figure 6). For 1 μ M concentrations of all three probes, negligible fluorescence enhancement was observed up to \sim 100 μ M Zn(II). For $Cu_2(FL2)$ and $Cu_2(FL2E)$, the Zn(II)-induced fluorescence enhancement remains minimal even at millimolar concentrations of $ZnCl_2$. For $Cu_2(FL2A)$, millimolar concentrations of Zn(II) induced a modest (\sim 8-fold) fluorescence enhancement, but one that is still less than one-third of that produced by NO. These data indicate that excess Zn(II) will not interfere with the NO-sensing properties of the Cu-FL probes in live cell or other applications.

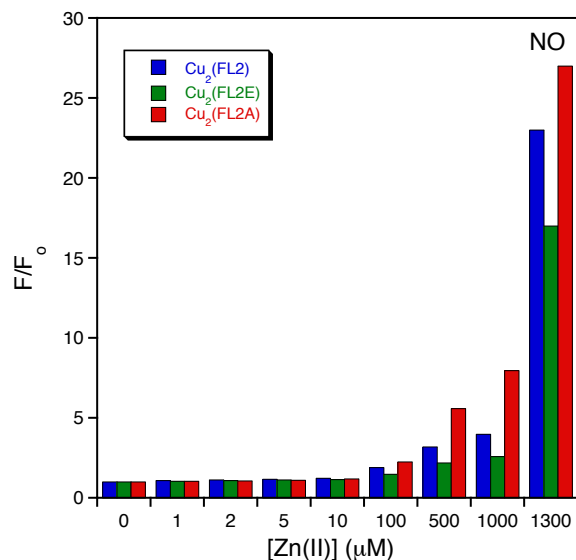


Figure 6. Selectivity of 1 μM $\text{Cu}_2(\text{FL2})$, 1 μM $\text{Cu}_2(\text{FL2E})$, and 1 μM $\text{Cu}_2(\text{FL2A})$ for NO over ZnCl_2 . Normalized fluorescence response after 1 h relative to the emission of the sensor in 50 mM PIPES, 100 mM KCl, pH 7, $T = 37^\circ\text{C}$.

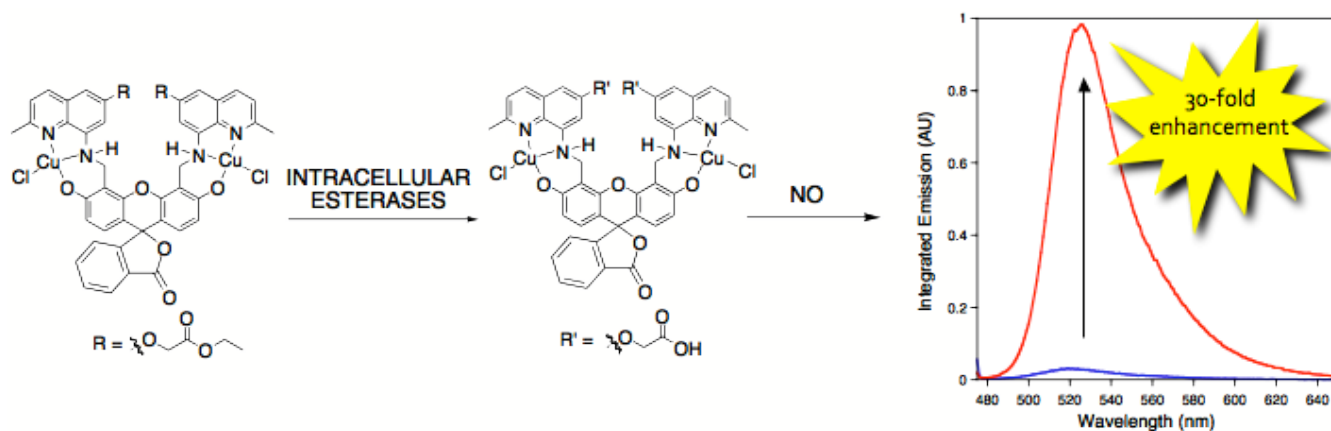
Summary

The synthesis and spectroscopic characterization of the fluorescein-based Cu(II) binding ligands FL2, FL2E, and FL2A are reported. These symmetrical constructs exhibit superior photophysical properties for NO sensing compared to the asymmetric FL1 probe. They are much less emissive in the off state ($\phi = 0.74 \pm 0.05\%$, $0.37 \pm 0.05\%$, and $1.8 \pm 0.2\%$ for FL2, FL2E, and FL2A, respectively, compared to $7.7 \pm 0.2\%$ for FL1) and therefore have larger dynamic ranges upon reaction with NO. The probes maintain their selectivity for NO over other biologically relevant RONS, and Zn(II) cannot displace Cu(II) to elicit a fluorescent response. The kinetics of NO-induced fluorescence enhancement was investigated, and approximate pseudo-first-order rate constants of $0.4 \pm 0.2 \text{ min}^{-1}$, $0.35 \pm 0.05 \text{ min}^{-1}$, and $0.6 \pm 0.1 \text{ min}^{-1}$ were obtained for reactions of $\text{Cu}_2(\text{FL2})$, $\text{Cu}_2(\text{FL2E})$, and $\text{Cu}_2(\text{FL2A})$ with NO, respectively, indicating that substitution of the aminoquinaldine unit does not significantly alter the rates.

Acknowledgement. This work was supported by grant CHE-0907905 from the National Science Foundation (NSF). Spectroscopic instrumentation at the MIT Department of Chemistry Instrument Facility is maintained with funding from NSF grants DBI-9729592 and CHE-9808061. We thank Drs. Michael Pluth, Zachary Tonzitech, and Elisa Tomat for insightful discussions.

Supporting Information Available: Mole-ratio plots from Cu(II) titrations of FL2E and FL2A; fits and residuals of pH titrations of FL2 and FL2A. This material is available free of charge via the Internet at <http://pubs.acs.org>.

TOC Graphic:



References

1. Furchgott, R. F.; Vanhoutte, P. M. *FASEB J.* **1989**, *3*, 2007-2018.
2. Ignarro, L. J.; Buga, G. M.; Wood, K. S.; Byrns, R. E.; Chaudhuri, G. *Proc. Natl. Acad. Sci. U. S. A.* **1987**, *84*, 9265-9269.
3. Rapoport, R. M.; Draznin, M. B.; Murad, F. *Nature* **1983**, *306*, 174-176.
4. Bogdan, C. *Nat. Immunol.* **2001**, *2*, 907-916.
5. Garthwaite, J. *Eur. J. Neurosci.* **2008**, *27*, 2783-2802.
6. Ignarro, L. J., *Nitric Oxide Biology and Pathobiology*. 1 ed.; Academic Press: San Diego, 2000.
7. Hetrick, E. M.; Schoenfisch, M. H. *Annu. Rev. Anal. Chem.* **2009**, *2*, 409-433.
8. Do, L.; Smith, R. C.; Tennyson, A. G.; Lippard, S. J. *Inorg. Chem.* **2006**, *45*, 8998-9005.
9. Smith, R. C.; Tennyson, A. G.; Lim, M. H.; Lippard, S. J. *Org. Lett.* **2005**, *7*, 3573-3575.
10. Smith, R. C.; Tennyson, A. G.; Won, A. C.; Lippard, S. J. *Inorg. Chem.* **2006**, *45*, 9367-9373.
11. Xing, C.; Yu, M.; Wang, S.; Shi, Z.; Li, Y.; Zhu, D. *Macromol. Rapid Commun.* **2007**, *28*, 241-245.
12. Kim, J.-H.; Heller, D. A.; Jin, H.; Barone, P. W.; Song, C.; Zhang, J.; Trudel, L. J.; Wogan, G. N.; Tannenbaum, S. R.; Strano, M. S. *Nat. Chem.* **2009**, *1*, 473-481.
13. Boon, E. M.; Marletta, M. A. *J. Am. Chem. Soc.* **2006**, *128*, 10022-10023.
14. Sato, M.; Hida, N.; Umezawa, Y. *Proc. Natl. Acad. Sci. U. S. A.* **2005**, *102*, 14515-14520.
15. Sato, M.; Nakajima, T.; Goto, M.; Umezawa, Y. *Anal. Chem.* **2006**, *78*, 8175-8182.
16. Lim, M. H.; Lippard, S. J. *Acc. Chem. Res.* **2007**, *40*, 41-51.
17. Richter-Addo, G. B.; Legzdins, P., *Metal Nitrosyls*. Oxford University Press: New York, 1992.
18. Hilderbrand, S. A.; Lippard, S. J. *Inorg. Chem.* **2004**, *43*, 5294-5301.
19. Soh, N.; Katayama, Y.; Maeda, M. *Analyst* **2001**, *126*, 564-566.
20. Hilderbrand, S. A.; Lippard, S. J. *Inorg. Chem.* **2004**, *43*, 4674-4682.
21. Franz, K. J.; Singh, N.; Spingler, B.; Lippard, S. J. *Inorg. Chem.* **2000**, *39*, 4081-4092.
22. Lim, M. H.; Kuang, C.; Lippard, S. J. *ChemBioChem* **2006**, *7*, 1571-1576.
23. Lim, M. H.; Wong, B. A.; Pitcock, W. H., Jr.; Mokshagundam, D.; Baik, M.-H.; Lippard, S. J. *J. Am. Chem. Soc.* **2006**, *128*, 14364-14373.
24. Lim, M. H.; Xu, D.; Lippard, S. J. *Nat. Chem. Biol.* **2006**, *2*, 375-380.
25. Lim, M. H.; Lippard, S. J. *J. Am. Chem. Soc.* **2005**, *127*, 12170-12171.
26. Lim, M. H.; Lippard, S. J. *Inorg. Chem.* **2006**, *45*, 8980-8989.
27. Ouyang, J.; Hong, H.; Shen, C.; Zhao, Y.; Ouyang, C.; Dong, L.; Zhu, J.; Guo, Z.; Zeng, K.; Chen, J.; Zhang, C.; Zhang, J. *Free Radical Biol. Med.* **2008**, *45*, 1426-1436.
28. Sarma, M.; Singh, A.; Gupta, G. S.; Das, G.; Mondal, B. *Inorg. Chim. Acta* **2010**, *363*, 63-70.
29. Tsuge, K.; DeRosa, F.; Lim, M. D.; Ford, P. C. *J. Am. Chem. Soc.* **2004**, *126*, 6564-6565.
30. Lim, M. H.; Lippard, S. J. *Inorg. Chem.* **2004**, *43*, 6366-6370.
31. Ortiz, M.; Torr ns, M.; Mola, J. L.; Ortiz, P. J.; Fragoso, A.; D az, A.; Cao, R.; Prados, P.; de Mendoza, J.; Otero, A.; Anti nolo, A.; Lara, A. *Dalton Trans.* **2008**, 3559-3566.
32. Hilderbrand, S. A.; Lim, M. H.; Lippard, S. J. *J. Am. Chem. Soc.* **2004**, *126*, 4972-4978.
33. Smith, R. C.; Tennyson, A. G.; Lippard, S. J. *Inorg. Chem.* **2006**, *45*, 6222-6226.
34. Gusarov, I.; Shatalin, K.; Starodubtseva, M.; Nudler, E. *Science* **2009**, *325*, 1380-1384.
35. Gusarov, I.; Starodubtseva, M.; Wang, Z.-Q.; McQuade, L.; Lippard, S. J.; Stuehr, D. J.; Nudler, E. *J. Biol. Chem.* **2008**, *283*, 13140-13147.
36. Parihar, M. S.; Parihar, A.; Chen, Z.; Nazarewicz, R.; Ghafourifar, P. *Biochim. Biophys. Acta* **2008**, *1780*, 921-926.
37. Parihar, M. S.; Parihar, A.; Villamena, F. A.; Vaccaro, P. S.; Ghafourifar, P. *Biochem. Biophys. Res. Commun.* **2008**, *367*, 761-767.
38. Patel, B. A.; Moreau, M.; Widom, J.; Chen, H.; Yin, L.; Hua, Y.; Crane, B. R. *Proc. Natl. Acad. Sci. U. S. A.* **2009**, *106*, 18183-18188.

39. Shatalin, K.; Gusarov, I.; Avetissova, E.; Shatalina, Y.; McQuade, L. E.; Lippard, S. J.; Nudler, E. *Proc. Natl. Acad. Sci. U. S. A.* **2008**, *105*, 1009-1013.
40. Tsien, R. Y. *Nature* **1981**, *290*, 527-528.
41. McQuade, L. E.; Ma, J.; Lowe, G.; Ghatpande, A.; Gelperin, A.; Lippard, S. J. *Proc. Natl. Acad. Sci. U. S. A.* **2010**, in press.
42. De La Rosa, M.; Kim, H. W.; Gunic, E.; Jenket, C.; Boyle, U.; Koh, Y.-H.; Korboukh, I.; Allan, M.; Zhang, W.; Chen, H.; Xu, W.; Nilar, S.; Yao, N.; Hamatake, R.; Lang, S. A.; Hong, Z.; Zhang, Z.; Girardet, J.-L. *Bioorg. Med. Chem. Lett.* **2006**, *16*, 4444-4449.
43. Burdette, S. C.; Walkup, G. K.; Spingler, B.; Tsien, R. Y.; Lippard, S. J. *J. Am. Chem. Soc.* **2001**, *123*, 7831-7841.
44. Brannon, J. H.; Magde, D. *J. Phys. Chem.* **1978**, *82*, 705-709.
45. Lim, M. D.; Lorković, I. M.; Ford, P. C. *Methods Enzymol.* **2005**, *396*, 3-17.
46. Burdette, S. C.; Frederickson, C. J.; Bu, W.; Lippard, S. J. *J. Am. Chem. Soc.* **2003**, *125*, 1778-1787.
47. Nolan, E. M.; Burdette, S. C.; Harvey, J. H.; Hilderbrand, S. A.; Lippard, S. J. *Inorg. Chem.* **2004**, *43*, 2624-2635.
48. Nolan, E. M.; Jaworski, J.; Okamoto, K.-I.; Hayashi, Y.; Sheng, M.; Lippard, S. J. *J. Am. Chem. Soc.* **2005**, *127*, 16812-16823.
49. Dive, C.; Cox, H.; Watson, J. V.; Workman, P. *Mol. Cell. Probes* **1988**, *2*, 131-145.
50. Leonhardt, H.; Gordon, L.; Livingston, R. *J. Phys. Chem.* **1971**, *75*, 245-249.
51. Vallee, B. L.; Falchuk, K. H. *Physiol. Rev.* **1993**, *73*, 79-118.
52. Frederickson, C. J.; Koh, J.-Y.; Bush, A. I. *Nat. Rev. Neurosci.* **2005**, *6*, 449-462.
53. Kröncke, K.-D.; Kolb-Bachofen, V. *Methods Enzymol.* **1999**, *301*, 126-135.